



Evidence of local superconductivity in granular Bi nanowires fabricated by electrodeposition

Mingliang Tian, Nitesh Kumar, and Moses H. W. Chan

Center for Nanoscale Science (MRSEC) and Department of Physics, The Pennsylvania State University, University Park, Pennsylvania 16802, USA

Thomas E. Mallouk

Center for Nanoscale Science (MRSEC) and Department of Chemistry, The Pennsylvania State University, University Park, Pennsylvania 16802, USA

(Received 15 April 2008; published 16 July 2008)

An unusual enhancement of resistance (i.e., a “superresistivity”) below a certain characteristic temperature T_{sr} was observed in granular Bi nanowires. This “superresistive” state was found to be dependent on the applied magnetic field as well as the excitation current. The suppression of T_{sr} by magnetic field resembles that of a superconductor. The observed superresistivity appears to be related to the nucleation of local superconductivity inside the granular nanowire without long-range phase coherence. The phenomenon is reminiscent of the “Cooper-pair insulator” observed previously in ultrathin two-dimensional superconducting films and three-dimensional percolative superconducting films.

DOI: [10.1103/PhysRevB.78.045417](https://doi.org/10.1103/PhysRevB.78.045417)

PACS number(s): 74.81.Bd, 74.78.Na, 73.63.Nm

I. INTRODUCTION

Bulk bismuth (Bi) has a rhombohedral crystal structure and displays semimetal properties down to at least 50 mK without showing evidence of superconductivity.^{1,2} Recently, we reported superconductivity in Bi nanowires with T_c of 7.2 and 8.3 K.³ These nanowires, fabricated by electrodepositing Bi into porous polycarbonate membranes, showed granular morphology consisting of crystalline rhombohedral Bi grains of a few nanometers to 15 nm. However, in spite of our effort in following similar fabrication conditions and protocols, superconductivity, with a sharp resistance drop at T_c , was found in only 18 out of a total of 38 samples studied. In contrast, the other 20 granular samples showed nonsuperconducting behavior down to 0.47 K. These contrast data obtained in granular Bi nanowires echoed the previous observation in literatures, i.e., superconductivity was seen in some granular films built of well-defined rhombohedral Bi nanoclusters in a variety of insulating matrices,^{4,5} but not seen in others, e.g., in the thermal evaporated or sputtered granular Bi films⁶ or in 6-nm-diameter crystalline or granular Bi nanowires confined in porous Vycor glass.⁷

To better understand the mechanism of superconductivity in granular Bi nanowires, structural or morphological studies were carried out by transmission electron microscopy (TEM) and electron diffraction (ED). Interesting contrast results were noticed between superconducting and nonsuperconducting granular nanowires. The rhombohedral grains in the superconducting wires were found to be aligned along the [001] direction within an angular distribution of 19°,³ while the grains in the nonsuperconducting nanowires showed random orientations. Because the transition temperatures of 7.2 and 8.3 K in superconducting wires are identical to those of the tetragonal high-pressure phases Bi-III (Refs. 8–11) and body-centered cubic Bi-V,^{8,9,12–14} we suggested that the grain boundaries between the grains with [001] orientation may assume the same crystal structures as those of Bi under high pressure due to structural reconstruction or local distortion.

The [001] alignment of the grains may allow a superconducting path along the atomically thin high-pressure phase percolating through at least one or a few granular wires in an array of wires embedded in the porous membrane. The high-pressure phases were not detected by x ray or TEM since the thickness of boundary layer is only on the order of a few atomic layers.

In this paper, we report a systematic study of the nonsuperconducting granular Bi nanowires. In the 20 nonsuperconducting granular wires we investigated, nine of them showed an unusual “super-resistive” behavior, specifically, an abrupt enhancement of resistance (R) below a well-defined temperature T_{sr} . The value of T_{sr} depends on the details of the sample and varies from sample to sample. The super-resistivity below T_{sr} was found to depend not only on the applied magnetic field (H) but also on the applied excitation current (I). By increasing H , T_{sr} is suppressed correspondingly and a phase boundary of the super-resistive state can be mapped out. For H exceeding a critical value H_{sr} , the enhanced resistance can be completely suppressed, resulting in a smooth semiconductor-type R - T curve from ~ 60 K down to 0.47 K. The H_{sr} - T phase boundary of the super-resistive state resembles that of a superconductor. The observed super-resistivity in granular Bi nanowires appears to be related to the nucleation of local superconductivity without the long-range phase coherence. The phenomenon is reminiscent of those reported in ultrathin two-dimensional (2D) granular Sn,¹⁵ Al,¹⁶ In, Ga, and Pb films,^{15,17} and three-dimensional (3D) granular Al (Ref. 18) and Al-Ge mixture films¹⁹ on the insulating side of the superconductor-insulator transition (SIT), as well as in percolative superconducting Pb films.^{20,21}

II. SAMPLE FABRICATION AND TRANSPORT MEASUREMENT

Granular Bi nanowires used in this work were made by electrochemically depositing Bi into commercially available

porous polycarbonate (PC) membranes at room temperature (the details of the fabrication process were described in Ref. 3). We found that the granular nanowires can be achieved with a deposition voltage between -2.0 and -3.5 V with a two electrode system. The diameter and length of the nanowires are controlled by the pore size and the thickness of the membrane.^{3,22,23} The actual diameter of the resulting nanowires is usually larger than the quoted pore size by manufacturers, the possible origins were discussed in literature.^{22,24} In this paper, all Bi nanowires have an actual diameter of 70 nm and a length (L) of 6 μm . Freestanding nanowires were obtained by dissolving the PC membrane in dichloromethane for TEM imaging.

Transport measurements were carried out on Bi nanowire arrays embedded in the PC membrane with a Physical Properties Measurement System, equipped with a ^3He insert and a superconducting magnet. Details about the transport measurements are reported earlier.^{25,26} The total resistance R of the system with this configuration consists of the contributions from the Bi nanowires, the metallic electrodes, and the point contacts between the electrodes and Bi nanowires. While the resistance of the metallic electrodes (i.e., Ag) is negligibly small (on the order of <0.1 Ω), the point-contact resistance of diameter (d) might not be negligible and can be estimated approximately by means of the Sharvin formula²⁷ $R_{\text{sh}}=4\rho_0\ell_e/3\pi d^2$, where ρ_0 is the resistivity of bulk Bi and ℓ_e is the electron mean-free path. Using $\rho_0\ell_e\sim 10^{-8}$ Ωcm^2 ,²⁸ R_{sh} is estimated to be 80 Ω for 70 nm Bi nanowires. This value is added to the total resistance as a series component to each Bi nanowire. If we make an assumption that the nanowires in each array are identical, the measured total resistance can be expressed as $R=(R_{\text{nw}}+2R_{\text{sh}})/N$, where R_{nw} is the resistance of each individual Bi nanowire in the array and N is the total number of the nanowires making contact with the electrodes. For a nanowire with $L=6$ μm and $d=70$ nm and taking a room-temperature resistivity value $\rho=315\sim 850$ $\mu\Omega\text{cm}$,²⁹ we get $R_{\text{nw}}=4\rho L/\pi d^2$ to be on the order of 4.9–13.3 k Ω at room temperature. Since $R_{\text{nw}}\gg R_{\text{sh}}$, the measured total resistance is dominated by the Bi nanowires.

III. EXPERIMENTAL RESULTS

Figure 1 shows the R vs T curves measured at zero magnetic field for the nine granular Bi nanowire samples showing the super-resistive behavior. Each sample is consisted of an array of nonintersecting 30–60 parallel wires making electrical contact to the electrodes. The value of the resistances is normalized at 100 K. All samples showed an anomaly at T_{sr} . Below T_{sr} , the resistance either increases sharply or displays a small drop first and then increases with decreasing temperature. The onset value of T_{sr} varies from sample to sample and four samples showed a T_{sr} at 7.1 ± 0.2 K or 8.1 ± 0.2 K, two samples at 3.6 ± 0.2 K, and three samples at 5.8 ± 0.2 K. It is interesting that each sample shows a sharp anomaly at a single T_{sr} , and the resistance at low temperatures shows a significant offset from the value extrapolated from $T>T_{\text{sr}}$. This means that the value of T_{sr} depends sensitively on the exact growth conditions during

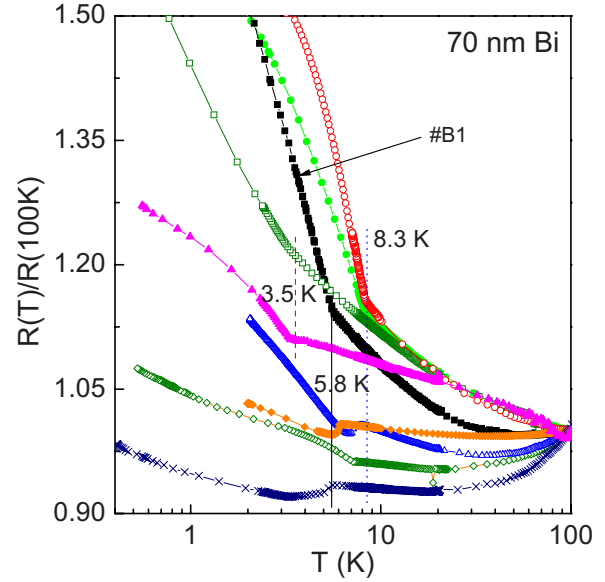


FIG. 1. (Color online) R vs T curves of nine granular Bi nanowire samples ($d=70$ nm, $L=6$ μm) showing a super-resistive behavior at a well-defined T_{sr} . Sample B1 shows a T_{sr} of 5.8 K, which will be discussed specifically in context.

the electrodeposition procedure, which we have not been able to completely manipulate or control from sample to sample. Other than different T_{sr} among different samples, all nine Bi nanowire samples show similar dependence on temperature, magnetic field, and excitation current. Here we focused our attention on one of these samples, namely, sample B1 with $T_{\text{sr}}=5.8\pm 0.2$ K. The typical TEM image of the sample B1 is shown in the inset of Fig. 2(a). This sample was deposited at a potential of -2.45 V and the nanowires show granular morphology with grain size ranging from a few nanometers up to 40 nm.

Figure 2(a) shows the R - T curves of sample B1 with an excitation current of 50 nA under perpendicular magnetic fields H of 0, 3.0, 4.0, 5.0, and 8.0 kOe. Since the measured total resistance $R=248$ Ω at 300 K, the number N of the wires in this array is estimated to be on the order of ~ 20 –54 using $\rho=315\sim 850$ $\mu\Omega\text{cm}$.²⁹ The R - T curves show a broad maximum near 200 K and insulating behavior below 60 K. Such a broad maximum in R is a common feature of semi-metallic Bi nanowires^{29–31} and can be understood as a consequence of the competition between the temperature dependence of the carrier concentration (n) and the carrier mobility (μ_0) in determining the resistivity $\rho=1/ne\mu_0$. While n decreases, μ_0 increases with decreasing temperature. Since n is nearly constant below 100 K, a metallic behavior or a saturation in resistance is expected at low temperatures. However, the situation in Bi nanowires is more complicated due to the finite-size effect,³⁰ weak-localization,^{7,32} and enhanced e - e interactions^{6,30} or other mechanism.^{33,34}

In sample B1, we found that under a magnetic field of $H=8.0$ kOe, the R - T curve shows a smooth insulating behavior from 60 K down to 0.42 K and its resistance $\ln R$ scales linearly with $T^{-1/2}$ between 2 and 55 K, shown in Fig. 2(b). This data can be expressed as $R=R_0\exp(T_0/T)^{1/2}$ with fitting parameters of $R_0=245$ Ω and $T_0=0.31$ K. The expo-

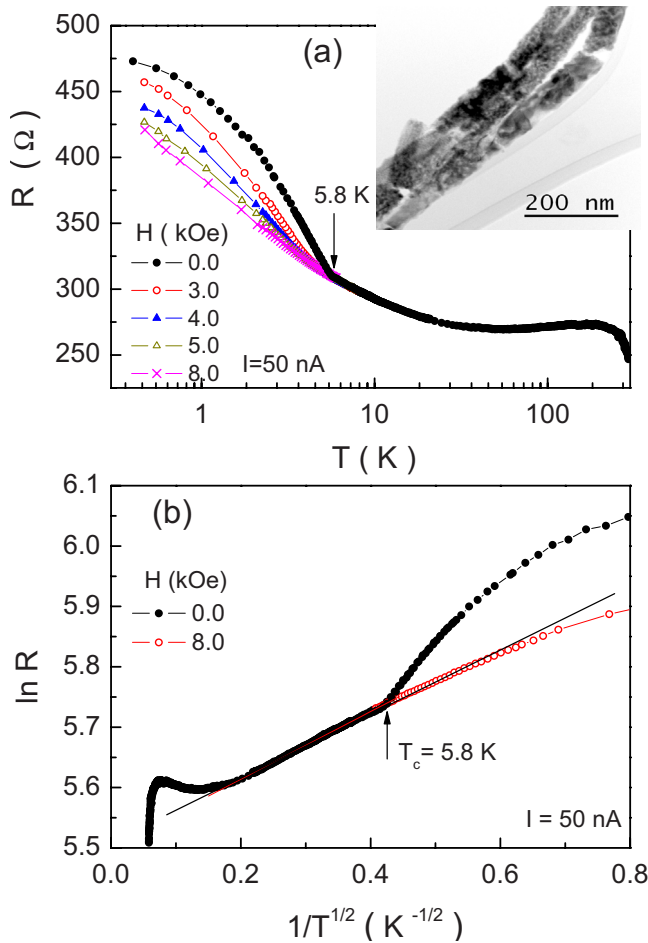


FIG. 2. (Color online) (a) R vs T curves of granular Bi nanowire sample B1 under different perpendicular magnetic fields H , measured with a small dc excitation current of 50 nA. The inset shows a TEM image of the wires. (b) $\ln R$ vs $1/T^{1/2}$ curves at two specific magnetic fields of $H=0$ and 8.0 kOe.

nential divergence in resistance is consistent with the model of strong localization with variable-range hopping (VRH) for a finite one-dimensional (1D) wire³⁵ or the Coulomb gap model of Efros-Shklovskii (ES).³⁶ The ES model is valid in both the 2D and 3D strong localization limits due to the Coulomb interaction. According to the VRH or ES model, the granular Bi sample B1 under a magnetic field of $H=8.0$ kOe is a “true insulator” below 60 K. At $H=5.0$ kOe and below, the measured resistance shows an abrupt enhancement below T_{sr} that rides on top of the smooth R - T curve obtained at $H=8.0$ kOe. The onset T_{sr} of the super-resistive behavior increases with decreasing H and it reaches 5.8 ± 0.2 K at $H=0$ Oe.

Figure 3(a) shows R vs H curves at different temperatures. For $T > 6.0$ K, a small positive magnetoresistance (MR) is found. Below 5.5 K, R - H curves show a plateau in the low-field region, and then a negative MR in higher field until a critical value H_{sr} before exhibiting the same positive MR behavior as observed for $T > 6.0$ K. The value of H_{sr} decreases with temperature and extrapolates to zero near 5.8 K. The overall feature of the R - T and R - H curves below 5.8 K is similar to that reported for a percolating superconducting Pb

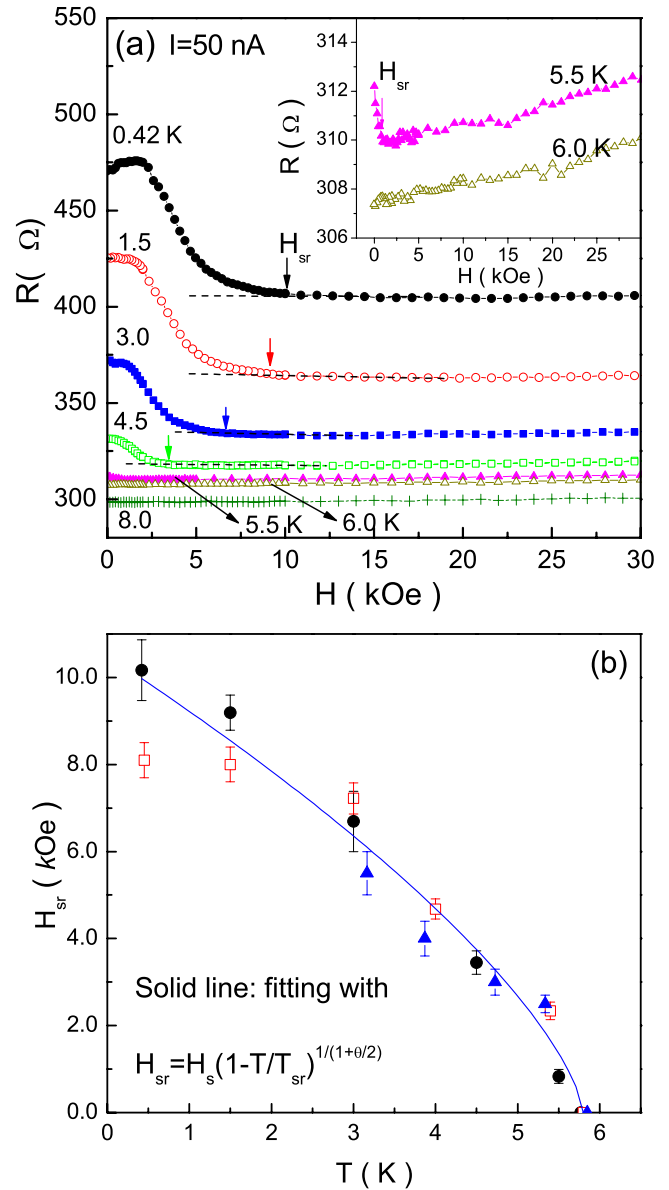


FIG. 3. (Color online) (a) R vs H curves of granular Bi nanowire sample B1, measured at different temperatures with a small dc excitation current of 50 nA. The inset is a blowup of the R - H curves at 5.5 and 6.0 K, respectively. (b) Phase diagram of H_{sr} vs T , obtained from the R - H and R - T curves shown in Figs. 3(a) and 4(b).

film below the percolation threshold,²⁰ and in granular Al-Ge mixture films on the insulating side of the SIT.¹⁹ These percolating granular films showed a nonsuperconducting behavior and a sharp resistance enhancement below the bulk T_c of Pb or Al at zero magnetic field. The features are similar to what we saw here in Figs. 1–3.

Similar super-resistive behavior was also observed in ultrathin 2D granular Sn,¹⁵ Al,¹⁶ In, Ga, and Pb films^{15,17} when the normal-state sheet resistance of the films was tuned to be on the order of the quantum resistance $R_Q = h/4e^2 = 6.4$ k Ω . The rapid increase of electrical resistance below the bulk T_c of granular superconducting films was interpreted as the consequence of the localized pairing of electrons without global phase coherence of the superconducting order parameter. In

other words, the super-resistive insulating state in these ultrathin granular films is not a true insulator, and the Cooper pairs are postulated to survive inside each individual grain. As a result, the conductivity is dominated by single-electron tunneling processes between the neighboring superconducting islands. The reduction of the gap in these superconducting islands by the application of a magnetic field results in a reduction of the resistance of the films, i.e., a negative MR effect. The similarity in the transport behavior of our granular Bi nanowires suggests that the observed super-resistivity below 5.8 K may have the same physical origin, namely, the existence of local superconducting islands without a long-range phase coherence.

Because the super-resistive behavior is always found below a specific temperature T_{sr} (shown in Figs. 1 and 2) and magnetic field H_{sr} [shown in Fig. 3(a)], a H_{sr} - T phase diagram, which defines such a boundary between super-resistive and normal, is shown in Fig. 3(b) as filled solid circles “●.” The value of H_{sr} is determined from Fig. 3(a) and defined from the point when the resistance deviates from the dashed linear baseline $\sim 0.7 \Omega$. The error bar of the H_{sr} is determined from the variation of H when the R deviates from the baseline $\sim 1.4 \Omega$ (the scattering of the R shown in the inset of Fig. 3(a) is less than 0.5Ω). The data points shown as open squares and solid triangles are deduced from different measurements and will be discussed below. The H_{sr} - T phase diagram resembles that of a 2D percolation superconducting film, where the temperature dependence of the upper critical magnetic field H_{c2} is predicted to follow the relation $H_{c2}(T) \propto \xi_s^{-2} \propto (T_c - T)^{1/(1+\theta/2)}$ with $\theta \sim 0.9$, when the percolation correlation length ξ_p becomes longer than the effective superconducting phase coherence length ξ_s .^{20,37} The solid line shown in Fig. 3(b) is a fit of the six data points shown as the filled solid circles according to the same formula, namely, $H_{sr}(T) = H_s(1 - T/T_c)^{1/(1+\theta/2)}$ with $\theta \sim 0.9$, $T_c = 5.8$ K, and a fitting parameter $H_s = 10.50 \pm 0.32$ kOe. The quality of the fit suggests that H_{sr} can be attributed to the upper critical field H_{c2} of a percolative superconductor. Above H_{sr} , the superconducting gap in each localized superconducting Bi island is completely destroyed and this leads to a smooth insulating R - T curve, which is consistent with a variable-range hopping process as shown in Fig. 2(b).

It is well known that the microscopic mechanism for superconducting to insulating transition (SIT) in a granular superconducting system is the competition between the intergrain charging energy (E_c) and the Josephson coupling energy (E_j) between neighboring grains. The system can either be in superconducting state ($E_j > E_c$) or in an insulating state ($E_c > E_j$), depending on the ratio of E_j/E_c . This mechanism, which usually explains the SIT in 2D granular films,^{15,17} Josephson junctions³⁸ or junction arrays,³⁹ and 3D granular system,¹⁹ was also applied to interpret the electrically insulating behavior in homogeneous films by Stewart *et al.*,⁴⁰ but the detailed picture for the local pairing in a homogeneous film remains unclear. When applying a dc bias onto such a Cooper-pair insulating system, one may expect that the charging energy E_c is to some extent, suppressed, and hence, a current-induced insulator to superconductor transition may appear due to the recovery of Josephson coupling. Such a current-induced effect is clearly seen in Fig. 4(a).

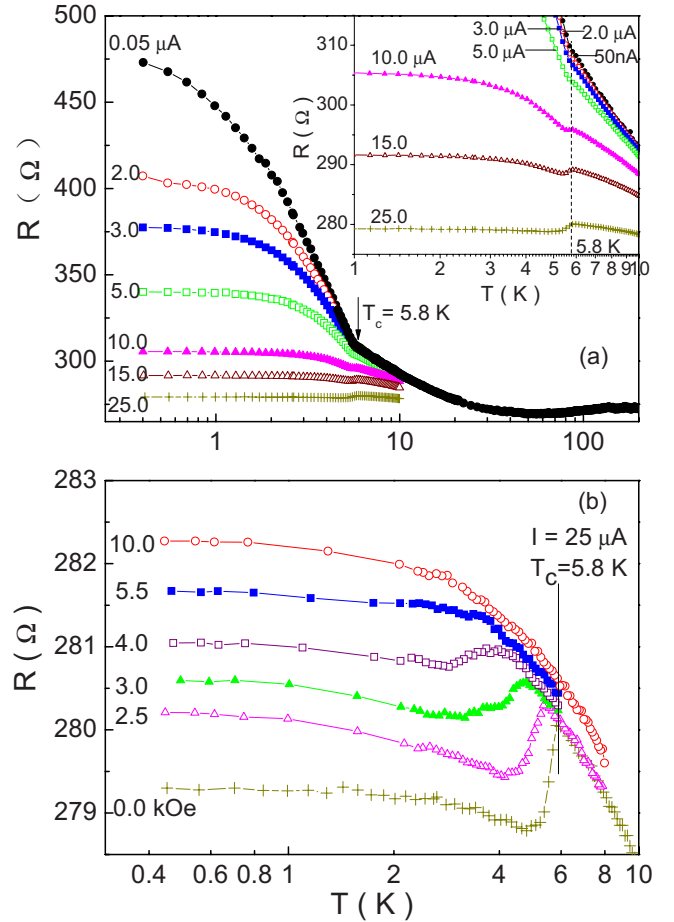


FIG. 4. (Color online) (a) R vs T of sample B1, measured with different dc excitation current. The inset is a blowup near the T_c . (b) R vs T curves under different H , measured with a higher dc current of $25 \mu\text{A}$.

Figure 4(a) shows the R - T curves measured at different dc excitation currents. With an excitation current of $I \leq 5.0 \mu\text{A}$, the R - T curves showed an upward kink at 5.8 K and a rapid increase in resistance below 5.8 K. At an excitation current of $10 \mu\text{A}$, a tiny resistance drop is found at 5.8 K prior to the appearance of the insulating behavior. The magnitude of the drop at 5.8 K increases with increasing dc bias [inset of Fig. 4(a)]. When $I = 25 \mu\text{A}$, the drop of the resistance from 5.8–0.42 K reaches at about 0.7% of the total normal-state resistance R_N (i.e., $\Delta R/R_N \sim 0.7\%$), and the R - T curve becomes nearly temperature independent below 5.8 K. This dc current-induced insulator to metal-like transition is not an artifact of the heating effect because the kink position at 5.8 K does not shift with the excitation current shown in the inset of Fig. 4(a).

Figure 4(b) shows the R - T curves measured with an excitation current of $25 \mu\text{A}$ under different perpendicular magnetic fields. The temperature T_{sr} at the kink decreases with increasing the applied H and finally becomes unresolvable at $H \geq 5.5$ kOe. This behavior resembles to that seen in a superconductor, where the critical temperature T_c is suppressed by an applied magnetic field. The phase boundary deduced from the kink position in Fig. 4(b) shown in Fig. 3(b) as solid triangles “▲,” is consistent with that defined from Fig.

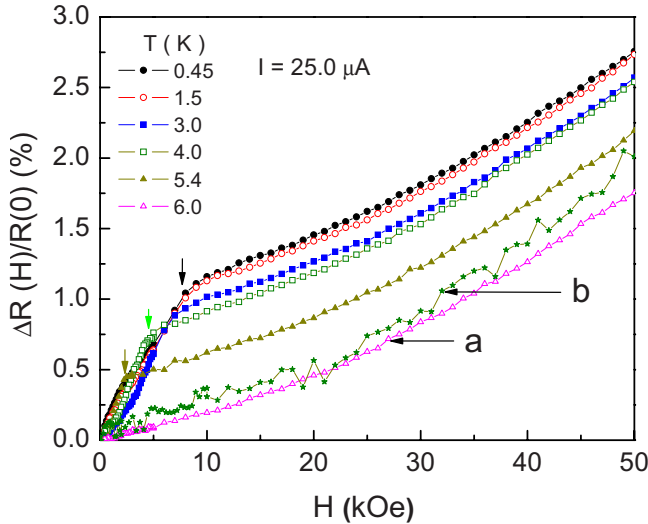


FIG. 5. (Color online) Magnetoresistance $\Delta R/R(0)$ vs H of sample B1 at different T , measured with a higher dc current, $25 \mu\text{A}$. A positive MR effect was seen, which is opposite to that shown in Fig. 3(a), measured with a small excitation current of 50 nA .

3(a). We thus attribute the current-induced tiny resistance drop at 5.8 K to the partial recovery of superconducting coupling between the localized superconducting islands. A similar current-induced insulator to superconductor transition was also reported by Wu *et al.*¹⁶ in an ultra thin granular Al film. They found that the granular Al film showed an insulating behavior when measured at a low excitation current of $I < 60 \text{ pA}$, but was superconducting at $I > 60 \text{ nA}$. The resistance drop reaches at about 90% of the normal-state resistance from T_c down to 0.4 K , which is much larger than that observed in granular Bi sample B1. The current-induced small resistance drop at T_{sr} in granular Bi nanowires provides an indication that the number of superconducting islands in B1 is likely very small and, therefore, the Josephson coupling between these islands is extremely weak even under a large dc bias.

We note that the total reduction of the wire resistance under an excitation current is unlikely to be due solely to the enhanced Josephson coupling between the superconducting islands. This is the case because the current dependent effect of the resistance was seen not only below T_{sr} but also above T_{sr} [shown in Fig. 4(a)]. Since the resistance above T_{sr} is due to single-electron hopping processes³⁵ between the strong localized states, the nonlinear dependence of the resistance on the excitation energy is expected, according to the VRH theory, when the excitation energy is larger than $k_B T$ [i.e., $dI/dV \sim \exp(V/k_B T)$ (Ref. 35)]. Hence, the substantial decrease of the total resistance below T_{sr} by increasing the current from 50 nA to $25 \mu\text{A}$ originates from both the VRH mechanism and the partial recovery of Josephson coupling between the localized pairing islands. A clear signature of the latter process is the tiny drop of the resistance at $5.8 \pm 0.2 \text{ K}$ under a large excitation current.

Figure 5 shows MR curves of $\Delta R/R(0)$ vs H , measured with a higher excitation current of $25 \mu\text{A}$ at different temperatures. At $T = 6.0 \text{ K}$, R increases smoothly with H and

this positive MR curve (labeled as “a”) is similar to that measured with a small excitation current of 50 nA at the same temperature, shown in curve “b” [i.e., the same curve that is shown in Fig. 3(a) at 6.0 K]. Both curves appear to collapse onto each other and, thus, indicate that the MR effect at $T > 6.0 \text{ K}$ is independent of the excitation current. We attribute this positive MR at $T > 6.0 \text{ K}$ to the normal galvanomagnetic MR due to the Lorenz force on electrons. It is worth noting that at $T < 5.8 \text{ K}$, the $\Delta R/R(0)$ - H curves measured at $25 \mu\text{A}$ showed an opposite behavior compared to those shown in Fig. 3(a). The MR, instead of being negative as in Fig. 3(a), is positive and the curves show a convex shape in the low-field region with a shoulder at a characteristic value indicated by the arrows. When the temperature increases, the shoulder position shifts to lower values of the magnetic field. If we define the magnetic field at the shoulder position as H_{sr} and then add the H_{sr} data into Fig. 3(b) as open squares “□,” we find that the phase boundary defined from Fig. 5 is in reasonable agreement with those defined from Fig. 3(a) and Fig. 4(b) within an uncertainty of 25%. These data indicate that the resistance shoulder in $\Delta R/R(0)$ - H curves measured at $25 \mu\text{A}$ probably corresponds to the upper critical field H_{c2} of the local superconducting islands.

IV. DISCUSSION

The above-mentioned experimental data provided an evidence that the super-resistivity of granular Bi nanowires below T_{sr} is due to the existence of local superconductivity. In contrast to granular Sn, In, Pb, or Al films, where their bulk materials are well-known superconductors, bulk rhombohedral Bi is not a superconductor. It is natural to wonder where the local superconductivity in granular Bi nanowires comes from.

In Ref. 3, we found that when the rhombohedral grains in these granular wires are oriented along the $[001]$ direction,³ the Bi nanowires showed complete superconducting, otherwise, the wires are nonsuperconducting or super-resistive if the grains are oriented randomly. By analysis of our previous structural and transport data, we have suggested that the superconductivity in granular Bi nanowires takes place along the boundaries between the $[001]$ aligned grains and, thus, allows superconducting path percolating through the boundaries. In contrast, the boundaries between grains that are randomly oriented are not superconducting. However, one cannot exclude the possibility that some local boundaries, which have some specific orientations (such as $[001]$ etc.), are superconducting, and thus leads to superconducting islands locally but do not form a global long-range phase coherence. As seen in Fig. 1, the samples showing an anomaly near 3.6 , 7.2 , or 8.3 K may correspond to the case of local superconductivity due to the formation of high-pressure phases Bi-II, III, and V, respectively (the observed T_c coincides with those of high-pressure Bi phase). What is then the origin of the T_c of $5.8 \pm 0.2 \text{ K}$ as seen in sample B1? It is known that thin amorphous Bi film has a T_c near $5.8 \sim 6.0 \text{ K}$ (Ref. 41) at zero magnetic field. The observed super-resistivity in B1 near $5.8 \pm 0.2 \text{ K}$ is very likely related to the nucleation of an

amorphous Bi islands residing at grain boundaries due to the strong disordering at the boundaries separated by nonsuperconducting crystalline rhombohedral Bi grains.

The above-mentioned scenario may explain why much previous research work on Bi nanowires or films showed great diversity in electrical properties. This is because the interfacial structures or the surface configurations of Bi nanowires or films are strongly related to the grain size, crystallinity, boundary condition, and the possible specific orientations between the grains, which all of them were affected by different growth techniques. For example, superconductivity was not seen in Bi nanowires fabricated by pressure injection of Bi into porous alumina membranes^{28,31–33} or Vycor glass,⁷ and in granular films fabricated by thermal evaporation or sputtering at low temperatures.⁶ In contrast, evidence of superconductivity was reported in some of rhombohedral single-crystal Bi nanowires ($T_c \sim 0.64$ K) fabricated by electrochemically deposition of Bi into porous polycarbonate membranes,⁴² in granular composite Bi films ($T_c < 5.0$ K) fabricated by codepositing Bi and matrix gas ($A = \text{Kr, Xe, O}_2, \text{ and H}_2$) onto cold substrates,^{4,5} and in single-crystalline Bi film deposited on a thin Ni films.⁴³ Although the T_c in these specific structures showed great diversity and the origins of the superconductivity remains unsolved, all of the data support such an idea that this “fickle” superconducting phenomenon is closely related to its surface configuration of grains (or wires) or the interfacial (or boundary) structures between the grains. In addition, recent magnetization study on a bulk Bi bicrystals with a large-angle ($>30^\circ$) twisting type crystallite interface⁴⁴ provided an evidence of two unknown superconducting phases with $T_c \sim 8.4$ K and ~ 4.3 K at the twisting interface.

Finally, we need to emphasize that, in addition to the 18 samples showing superconductivity and nine samples showing super-resistivity, we still have 11 samples showing a smooth insulating behavior down to 0.47 K. Since our measurements were performed on nanowire arrays, the experiments do not allow us to quantitatively determine whether the observed smooth insulating behavior is due to the absence of local pairs. If a small number of local pairs survive only in some of the granular wires in the array, they may not show up in resistance measurement under a parallel configuration of nanowires.

V. SUMMARY

We report an unusual super-resistive phenomenon in granular Bi nanowires that appears to be due to the nucleation of local superconductivity without global phase coherence. The phenomenon is reminiscent to those observed previously in ultrathin 2D superconducting films and 3D percolative superconducting films. Our data clearly indicate that the transport properties of Bi nanostructures are exceptionally sensitive to their specific configurations, they can be superconducting, super-resistive, or insulating, and strongly dependent on the exact local structures or configurations at grain boundaries or surface, as well as the structural orientations between the grains.

ACKNOWLEDGMENTS

We acknowledge helpful discussions with J. Jain, Y. Liu, and J. G. Wang. This work was supported by the Center for Nanoscale Science (Penn State MRSEC) funded by NSF under Grant No. DMR-0213623.

-
- ¹J. P. Issi, *Aust. J. Phys.* **32**, 585 (1979).
²F. Y. Yang, K. Liu, K. Hong, D. H. Reich, P. C. Searson, and C. L. Chien, *Science* **284**, 1335 (1999).
³M. L. Tian, J. G. Wang, N. Kumar, T. H. Han, Y. Kobayashi, T. E. Mallouk, and M. H. W. Chan, *Nano Lett.* **6**, 2773 (2006).
⁴B. Weitzel and H. Micklitz, *Phys. Rev. Lett.* **66**, 385 (1991); B. Weitzel, A. Schreyer, and H. Micklitz, *Europhys. Lett.* **12**, 123 (1990).
⁵C. Vossloh, M. Holdenried, and H. Micklitz, *Phys. Rev. B* **58**, 12422 (1998).
⁶D. E. Beutler and N. Giordano, *Phys. Rev. B* **38**, 8 (1988).
⁷T. E. Huber and M. J. Graf, *Phys. Rev. B* **60**, 16880 (1999).
⁸O. Degtyareva, M. I. McMahon, and R. J. Nelmes, *High Press. Res.* **24**, 319 (2004).
⁹H. Iwasaki, J. H. Chen, and T. Kikegawa, *Rev. Sci. Instrum.* **66**, 1388 (1995).
¹⁰B. Brandt and N. I. Ginzburg, *Sov. Phys. JETP* **12**, 1082 (1961); **17**, 326 (1963).
¹¹H. D. Stromberg and D. R. Stephens, *J. Phys. Chem. Solids* **25**, 1015 (1964).
¹²T. T. Chen, J. T. Chen, J. D. Leslie, and H. J. T. Smith, *Phys. Rev. Lett.* **22**, 526 (1969).
¹³N. B. Brandt and N. I. Ginzburg, *Contemp. Phys.* **10**, 355 (1969).
¹⁴J. Wittig, *Z. Phys.* **195**, 215 (1966).
¹⁵D. B. Haviland, H. M. Jaeger, B. G. Orr, and A. M. Goldman, *Phys. Rev. B* **40**, 719 (1989); B. G. Orr, H. M. Jaeger, and A. M. Goldman, *ibid.* **32**, 7586 (1985).
¹⁶W. H. Wu and P. W. Adams, *Phys. Rev. B* **50**, 13065 (1994); *Phys. Rev. Lett.* **73**, 1412 (1994).
¹⁷R. P. Barber, Jr., L. M. Merchant, A. La Porta, and R. C. Dynes, *Phys. Rev. B* **49**, 3409 (1994).
¹⁸M. Kunchur, Y. Z. Zhang, P. Lindenfeld, W. L. McLean, and J. S. Brooks, *Phys. Rev. B* **36**, 4062 (1987).
¹⁹A. Gerber, A. Milner, G. Deutscher, M. Karpovsky, and A. Gladkikh, *Phys. Rev. Lett.* **78**, 4277 (1997).
²⁰A. Gerber and G. Deutscher, *Phys. Rev. Lett.* **63**, 1184 (1989); A. Kapitulnik and G. Deutscher, *ibid.* **49**, 1444 (1982).
²¹J. Wang, X. C. Ma, Y. Qi, Y. S. Fu, S. H. Ji, L. Lu, J. F. Jia, and Q. K. Xue, *Appl. Phys. Lett.* **90**, 113109 (2007).
²²M. L. Tian, J. G. Wang, J. Kurtz, T. E. Mallouk, and M. H. W. Chan, *Nano Lett.* **3**, 919 (2003).
²³J. G. Wang, M. L. Tian, N. Kumar, and T. E. Mallouk, *Nano Lett.* **5**, 1247 (2005).
²⁴Z. L. Xiao, C. Y. Han, U. Welp, H. H. Wang, W. K. Kwok, G. A. Willing, J. M. Hiller, R. E. Cook, D. J. Miller, and G. W. Crab-

- tree, *Nano Lett.* **2**, 1293 (2002).
- ²⁵M. L. Tian, J. G. Wang, J. S. Kurtz, Y. Liu, M. H. W. Chan, T. S. Mayer, and T. E. Mallouk, *Phys. Rev. B* **71**, 104521 (2005); M. L. Tian, J. G. Wang, J. Snyder, J. Kurtz, Y. Liu, P. Schiffer, T. E. Mallouk, and M. H. W. Chan, *Appl. Phys. Lett.* **83**, 1620 (2003).
- ²⁶M. L. Tian, N. Kumar, S. Y. Xu, J. G. Wang, J. S. Kurtz, and M. H. W. Chan, *Phys. Rev. Lett.* **95**, 076802 (2005); M. Tian, N. Kumar, J. Wang, S. Xu, and M. Chan, *Phys. Rev. B* **74**, 014515 (2006).
- ²⁷Y. V. Sharvin, *Sov. Phys. JETP* **21**, 655 (1965).
- ²⁸T. E. Huber, K. Celestine, and M. J. Graf, *Phys. Rev. B* **67**, 245317 (2003).
- ²⁹T. W. Cornelius, M. E. Toimil-Molares, R. Neumann, and S. Karim, *J. Appl. Phys.* **100**, 114307 (2006).
- ³⁰Z. B. Zhang, X. Z. Sun, M. S. Dresselhaus, J. Y. Ying, and J. Heremans, *Phys. Rev. B* **61**, 4850 (2000).
- ³¹J. Heremans and C. M. Thrush, *Phys. Rev. B* **59**, 12579 (1999).
- ³²J. P. Heremans, C. M. Thrush, Z. Zhang, X. Sun, M. S. Dresselhaus, J. Y. Ying, and D. T. Morelli, *Phys. Rev. B* **58**, R10091 (1998).
- ³³T. E. Huber, A. Nikolaeva, D. Gitsu, L. Konopko, and M. J. Graf, *Physica E (Amsterdam)* **37**, 194 (2007).
- ³⁴A. Nikolaeva, D. Gitsu, L. Konopko, M. J. Graf, and T. E. Huber, *Phys. Rev. B* **77**, 075332 (2008).
- ³⁵P. A. Lee, *Phys. Rev. Lett.* **53**, 2042 (1984).
- ³⁶A. L. Efros and B. I. Shklovskii, *J. Phys. C* **8**, L49 (1975).
- ³⁷A. Gerber and G. Deutscher, *Phys. Rev. B* **35**, 3214 (1987).
- ³⁸J. S. Penttila, U. Parts, P. J. Hakonen, M. A. Paalanen, and E. B. Sonin, *Phys. Rev. Lett.* **82**, 1004 (1999).
- ³⁹H. S. J. van der Zant, W. J. Elion, L. J. Geerligs, and J. E. Mooij, *Phys. Rev. B* **54**, 10081 (1996).
- ⁴⁰M. D. Stewart, Jr., A. Yin, J. M. Xu, and J. M. Valles, Jr., *Science* **318**, 1273 (2007).
- ⁴¹S. Chakravarty, S. Kivelson, G. T. Zimanyi, and B. I. Halperin, *Phys. Rev. B* **35**, 7256 (1987).
- ⁴²Z. X. Ye, H. Zhang, H. D. Liu, W. H. Wu, and Z. P. Luo, *Nanotechnology* **19**, 1 (2008).
- ⁴³J. S. Moodera and R. Meservey, *Phys. Rev. B* **42**, 179 (1990).
- ⁴⁴F. M. Muntyanu, A. Gilewski, K. Nenkov, J. Warchulska, and A. J. Zaleski, *Phys. Rev. B* **73**, 132507 (2006).